Environmental Stress Cracking Behavior of Short-Chain Branch Polyethylenes in Igepal Solution Under a Constant Load

J. T. YEH,* JUNG-HORNG CHEN, and HUEI-SONG HONG

Department of Textile Engineering, National Taiwan Institute of Technology, Taipei, Taiwan 106, Republic of China

SYNOPSIS

An investigation of the influence of branch length and crystallinity on environmental stress cracking properties of short-chain branch polyethylenes (SBPEs) in Igepal solution is reported. The precise value of Igepal transition time (ITT) and difference between the failure process of SBPEs in air and in Igepal solution were determined by comparing their plots of notch opening displacements vs. time in air and in Igepal solution. Igepal transition time can only be found as the failure time (t_{fl}) is greater than the critical time Igepal required to "accelerate" the fracture of SBPEs in Igepal solution. Prior to ITT, time dependence of notch opening displacements and fracture surfaces of samples in Igepal solution were similar to those in air. In contrast, obvious voids appeared in the base of craze and crazelike structures containing clear voids were found on the fracture remnants of samples with t_{fl} longer than their ITTs. The value of ITT and t_{fl} were found to increase significantly for samples associated with higher crystallinity. However, no significant difference in value of ITT was found for samples with the same crystallinity, tie-molecule density, molecular weight, branch frequency, but different branch length. Finally, environmental stress cracking resistance (ESCR) and t_{fl} of SBPEs in Igepal solution increased dramatically as the short-chain branch length increased. This dramatic improvement in environmental stress cracking properties with short-chain branch length is attributed to the increasing sliding resistance of the polymer chains through the crystal and through the entanglement in amorphous region at time before and after ITT. © 1994 John Wiley & Sons, Inc.

INTRODUCTION

The failure time of static fatigue (t_{fa})[1-3] and fracture toughness[4] of short-chain branch polyethylene (SBPE) in air were found to improve more significantly than those of low-density and high-density polyethylene polymers. This dramatic improvement in t_{fa} has been attributed to the presence of short-chain branches in the molecules of polyethylenes, which results in an increasing tie-molecule density and, hence, an increasing resistance of pulling a molecule through the crystalline region than that of a smooth molecule.[1] More detailed investigations[5-7] indicated that the length and frequency of the short-chain branches have a profound effect on the static fatigue properties of SBPEs. For instance, t_{fa} was found to increase approximately 10,000 times when the butyl branch frequency of the ethylene–hexene copolymers increases from 0 butyl branch/1000 carbon atoms to 4.6 butyl branches/1000 carbon atoms.[5] Recently, a profound effect of short-chain branch length on static fatigue properties of SBPE polymers was found in our laboratories.[7] In our previous study, various thermal histories were utilized to generate samples with the same crystalline microstructure (i.e., percent crystallinity, spherulite size, lamellar thickness, and tie-molecule density) for a series of SBPEs with similar weight-average molecular weight, molecular weight distribution, branch frequency, but different short-chain branch lengths. The effect of branch length has been isolated and found to have a beneficial influence on the

* To whom correspondence should be addressed.

Journal of Applied Polymer Science, Vol. 54, 2171–2186 (1994)
 CCC 0021-8995/94/132171-16

static fatigue properties of SBPE polymers. The static fatigue test can provide a reliable way for evaluating the performing lifetime of SBPEs, however, in the neighborhood of room temperature, it usually takes too long. In fact, t_{fa} may be up to several years for good-quality pipe resins even if the test temperature is elevated.[8] Industry needs a relatively short-time test for assessing the slow crack growth behavior of these good-quality resins.[9] The test of environmental stress cracking resistance (ESCR) of polyethylene (PE) in Igepal solution was developed to meet these requirements, which should be capable of producing the slow crack growth process as the same process that occurs when a polyethylene gas pipe fails in service after a long period of time.[9,10]

However, as far as we know, only few investigations[9-11] on environmental stress cracking properties of SBPEs in Igepal solution have been reported in the literature. By focusing on these few publications,[9-11] a profound effect of the short-chain branch length on environmental stress cracking properties of SBPEs was found. Bubeck and Baker[11] found that the failure time (t_{fl}) in Igepal solution of SBPEs at a fixed density and a melt index increased significantly as the branch length increased from 1 to 6 carbon lengths. Recently, Ward and coauthors[9,10] found that the failure time of SBPEs in Igepal solution (t_{fl}) was considerably smaller than that in air (t_{fa}) as t_{fl} is greater than a critical value ($\sim$ 1000 min). However, no significant difference between t_{fl} and t_{fa} was observed, when t_{fl} is shorter than the critical value of time. They called the critical time for failure as the Igepal transition time (ITT), and found that ITT decreased with increasing temperature. Obviously, Igepal requires a certain amount of time to interact with the polymer before it becomes "effective," and was suggested[9] to relate to the diffusion coefficient of the Igepal into the crystalline region of polyethylene. This critical time required to accelerate the stress cracking of polyethylenes in Igepal solution was the first time reported in the literature. In addition to the short-chain branch effect, molecular weight[12] and degree of crystallinity[13] were also found to exhibit a beneficial influence on the ESCR of PE in Igepal solution. Unfortunately, it is not yet fully understood how these factors affect the ITT and the mechanism whereby Igepal accelerates the failure of SBPE.

In this present report, the value of ITT was determined by comparing the plots of notch opening displacements vs. time of SBPE samples loaded in air and in Igepal solution. By doing so, the precise value of ITT and the difference between the failure process of SBPEs in air and in Igepal solution can be obtained. Samples with the same crystallinity, tie-molecule density, molecular weight, branch frequency, but different branch lengths were utilized to investigate the effect of branch length on ITT and other environmental stress cracking properties of SBPE polymers. Additional efforts were made to prepare samples with the same molecular structure (i.e., molecular weight, branch length, and branch frequency) but different crystallinities. In this way, the effects of crystallinity on ITT and other environmental stress cracking properties of SBPEs can be studied.

Table I. Thermal Histories and Properties of Short-Chain Branch Polyethylenes

Sample		Thermal Histories	Comonomer	M_w	MWD	Branch Frequency (Number of Branches/ 1000 Carbon Atoms)	Branch Type
A	A_1	Isothermal crystallization at 100°C/12 h					
	A_2	Isothermal crystallization at 115°C/1 h	1-Butene	9.2×10^4	3.4	18	Ethyl
	A_3	Quenched at −15°C/20 min					
B	B_1	Isothermal crystallization at 90°C/1 h					
	B_2	Isothermal crystallization at 115°C/1 h	1-Hexene	9.4×10^4	3.3	18	Butyl
	B_3	Quenched at −15°C/20 min					
C	C_1	Isothermal crystallization at 100°C/1 h					
	C_2	Isothermal crystallization at 115°C/1 h	1-Octene	9.7×10^4	3.6	18	Hexyl
	C_3	Quenched at −15°C/20 min					

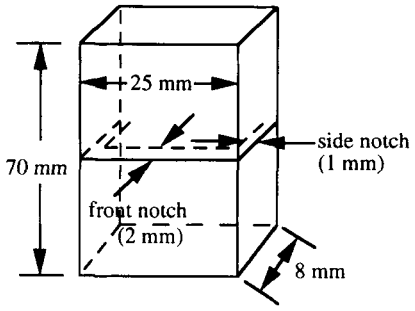

Figure 1 Shape and dimension of the single-edge notched tensile specimen.

EXPERIMENTAL

Materials and Preparation

Three commercial SBPE resins were selected for this study. These samples have similar molecular weight, molecular weight distribution, and, as will be shown later, similar branch frequency, but different branch length. The molecular weight, molecular weight distribution, and type of comonomer of each sample are listed in Table I. The thermal histories determined in our previous study[7] were used to generate samples A_1, B_1, and C_1 with approximately the same crystallinity and tie-molecule density and are summarized in Table I. Efforts were also made to prepare samples (i.e., samples A_2, A_3, B_2, B_3, C_2, and C_3) of different crystallinity by using other thermal histories. As mentioned previously, the purpose of doing this is to study the possible effects of crystallinity on ITT and other environmental stress cracking properties of SBPE polymers in Igepal solution. Prior to sample preparation, these resins were dried in an oven at 80°C for 1 h. The dried resins were molded using an injection molding machine to a rectangular die with dimensions of 75

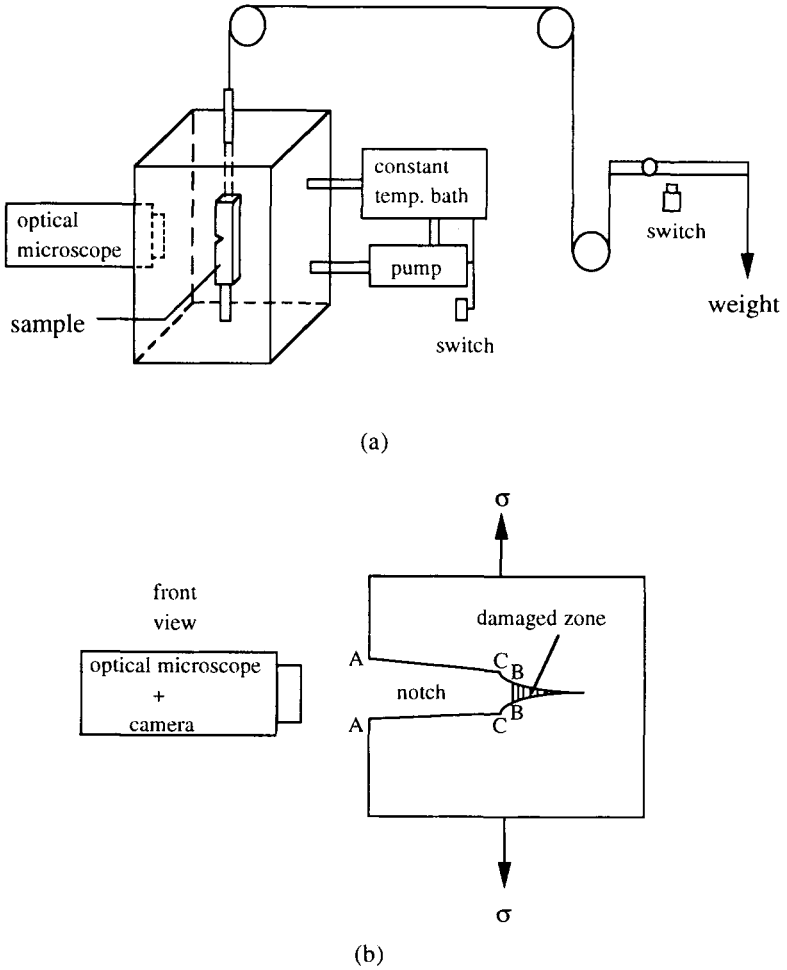

Figure 2 (a) Apparatus of environmental stress cracking tests. (b) Experimental measurement of notch opening displacements.

Table II. Microstructural Characterization Associated with Each Sample

Sample		Thermal Histories	W_c (%)	f_T (%)	$T(M)$
A	A_1	Isothermal crystallization at 100°C/12 h	40	6.3	26.0
	A_2	Isothermal crystallization at 115°C/1 h	42	6.3	25.9
	A_3	Quenched at −15°C/20 min	26	6.5	27.3
B	B_1	Isothermal crystallization at 90°C/1 h	40	6.2	26.0
	B_2	Isothermal crystallization at 115°C/h	42	6.2	25.8
	B_3	Quenched at −15°C/20 min	27	6.4	26.9
C	C_1	Isothermal crystallization at 100°C/1 h	41	6.0	26.3
	C_2	Isothermal crystallization at 115°C/1 h	43	6.0	26.1
	C_3	Quenched at −15°C/20 min	27	6.2	27.0

× 80 × 10 mm at various temperatures for various amounts of time. The molded samples were then air cooled to 35°C after the required crystallization time.

Characterization

Branch Length and Branch Frequency

The branch length and frequency of each sample were determined by using Bruker MSL-200 ^{13}C-NMR spectrometer operating at 50 MHz. Polymer solutions for ^{13}C-NMR measurements was prepared in 1,2-dichlorobenzene with concentrations maintained at 0.43 g/mL. Prior to examination, the sample was transferred into a 10-mm NMR sample tube and then heating at 150°C for 3–4 h. All spectra were obtained at 130°C. The branch frequencies of samples A, B, and C estimated from ^{13}C-NMR are approximately 18.0 branches/1000 carbon atoms.[14] In addition, the results obtained from ^{13}C-NMR spectra of all samples suggested that samples A, B, and C are associated with ethyl, butyl, and hexyl short-chain branches, respectively (see Table I).

Molecular Weight and Molecular Weight Distribution

The molecular weight and its distribution associated with SBPEs were carried out using a Viscotek gel permeation chromatography (GPC). The samples were prepared by dissolving in pure decahydronaphthalin ($C_{10}H_{18}$) at 135°C to reach a final concentration of 1.0 mg/mL. The amount injected was 0.1 mL and the solvent flowed 1 mL/min at 135°C. The results of weight-average molecular weight (M_w) and molecular weight distribution (MWD) calculated from GPC were summarized in Table I.

Thermal Analysis

The thermal behavior was estimated from the melting endotherm in differential scanning calorimetry (DSC) curves; DSC measurements were carried out with a DuPont 2000 thermal analyzer calibrated with an indium standard. Each sample, weighing 10 mg, was placed in a standard aluminum sample pan. All scans were carried out at a constant heating rate of 20°C/min.[15]

Tie-Molecule Density

The measurements of tie molecules have been proposed with many techniques to measure transmission electron microscopy,[16–23] neutron scattering,[24] nuclear magnetic resonance,[25] etc. However, due to the small dimensions and complexity of the inter-

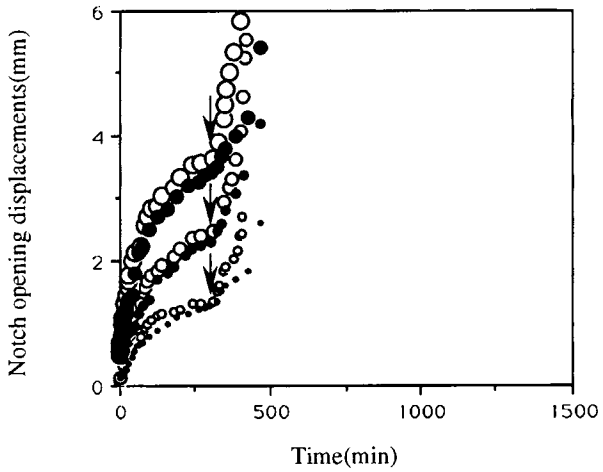

Figure 3 Notch opening displacements against time of sample A_1 fractured in air: (○) BB, (○) CC, (○) AA; and in Igepal solution: (●) BB, (●) CC, (●) AA, at 9 MPa. Arrow indicates δ_c.

crystalline links, these techniques do not appear to be suitable for ready analysis of a relatively large number of bulk samples. To measure the number of tie molecules of bulk polymer, Brown and Ward[26] presented an equation for calculating the number of tie molecules in terms of the low-temperature fracture stress. Recently, Yeh and Runt[27] suggested using chain dimension of the polymers to estimate the number of tie molecules. In this study, tie-molecule density was evaluated from brittle tensile strength measurement and/or predicted from the chain dimension. We are not suggesting that the brittle fracture stress or the chain dimension approach provides a precise measurement of tie-molecule density but rather qualitative information that will allow a comparison between various samples of a given polymer. The brittle tensile strength of dog-bone-shaped specimens was done with a material test system (MTS) using a crosshead speed of 50 cm/min at a temperature of about −110°C. In this study, four or more duplicate samples of each specimen type were tested and averaged.

Environmental Stress Cracking Experiments

The single-edge notched specimens were sectioned and polished from the injection-molded plaques. The geometry of the specimen is shown in Figure 1. Each

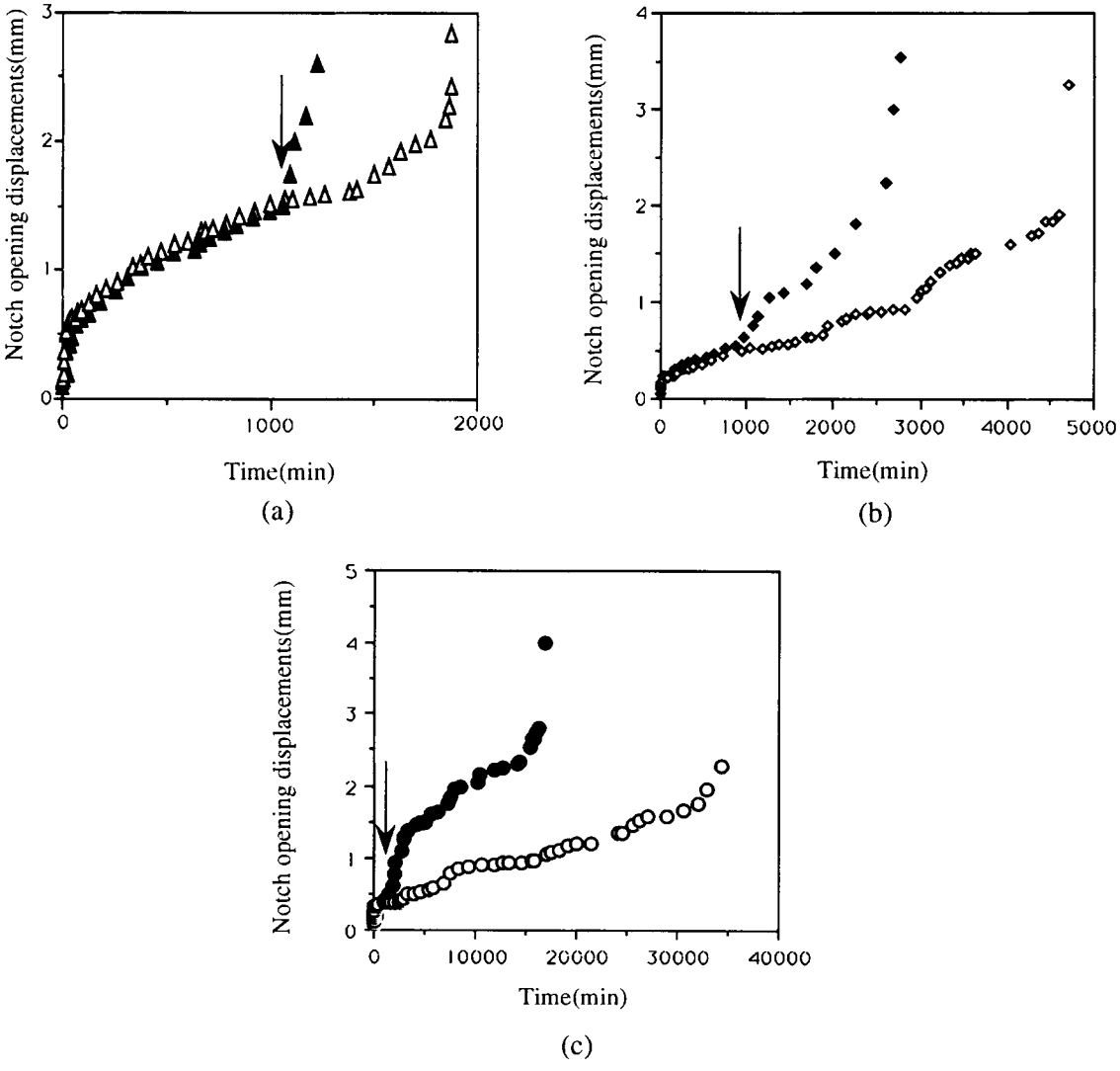

Figure 4 Notch opening displacements against time: (a) sample A_1 in (△) air and in (▲) Igepal solution; (b) sample B_1 in (◇) air and in (◆) Igepal solution; (c) sample C_1 in (○) air and in (●) Igepal solution at 8.5 MPa, arrow indicates ITT.

Table III. Igepal Transition Time (ITT) and Failure Time (t_{fI}) of All Samples

Stress (MPa) ITT and t_{fI} (min) Sample	9 MPa		8.5 MPa		8 MPa	
	ITT	t_{fI}	ITT	t_{fI}	ITT	t_{fI}
A_1	Not found	480	1040	1280	1020	4030
A_2	Not found	570	1060	1530	1080	4470
A_3	Not found	310	510	640	560	2510
B_1	Not found	670	1020	2010	980	6720
B_2	Not found	860	1140	2920	1180	9380
B_3	Not found	690	610	1610	590	5360
C_1	1060	4790	1070	17050	1100	359160
C_2	1080	6200	1130	22140	1140	—
C_3	620	3480	590	11050	640	—

notch was made with a fresh razor blade by pressing it into the specimen at a constant speed of 50 μm/min. The design of dimensions of the specimen took into account the following factors. The width of the specimen is chosen to be 25 mm so that, with aid of the side grooves, the fracture occurs under practically pure plain strain conditions.[6,7] The single-edge notched specimen was then placed in the apparatus shown schematically in Figure 2(a) and immersed in a 10% solution of Igepal CO-630. Before constant loading tests, all samples were presoaked in Igepal solution for 2 h. The specimen was then loaded under a constant stress and the temperature was controlled at 25 ± 1°C. The notch opening displacements (COD) at the following three locations were measured with an Olympus SZ40 optical microscope: (1) at the surface of the specimen (AA), (2) at the root of the notch as formed by razor blade (CC), and (3) at the base of the craze (BB) [see Fig. 2(b)]. The loading stress, σ, used in this study was calculated as following:

$$\sigma = \frac{F}{A}$$

where F is the applied load and A is the notched cross-sectional area.

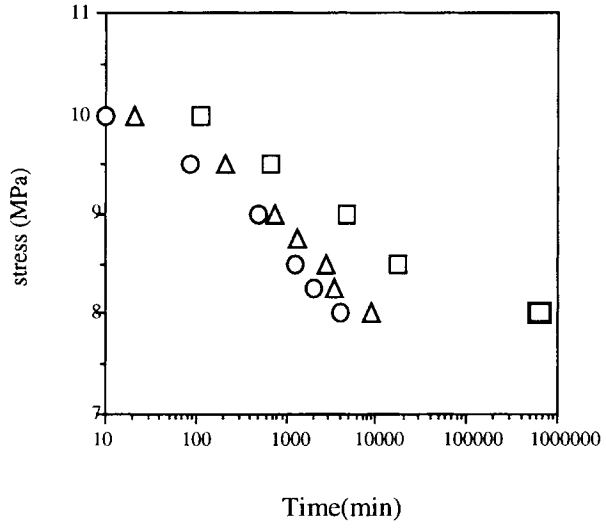

Figure 5 Loading stress vs. failure time (t_{fI}) for SBPEs in Igepal solution: (○) sample A_1, (△) sample B_1, (□) sample C_1.

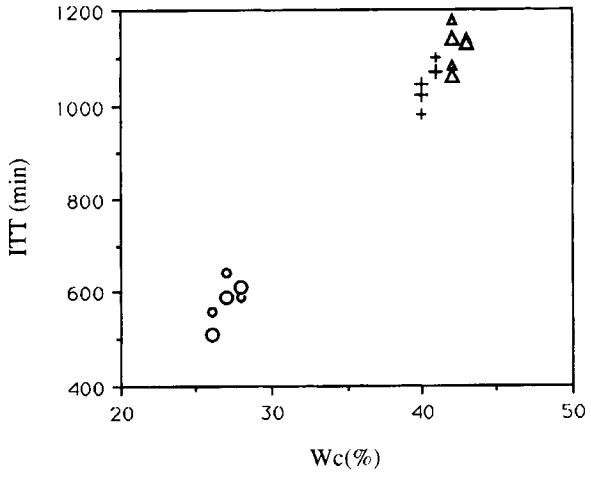

Figure 6 ITT of samples of series 1 at (+) 8 MPa; series at 1 (+) 8.5 MPa; series 2 at (△) 8 MPa; series 2 at (△) 8.5 MPa; series 3 at (○) 8 MPa; series 3 at (○) 8.5 MPa.

Morphology of the Notched Root and Fracture Surface Analysis

The morphological changes of all samples fractured in Igepal solution and in air were observed using an Olympus SZ40 optical microscope from the outlook of the roots. Photographs were made before and after ITT for sample loaded in air and Igepal solution, by which the possible change in morphology of the roots due to Igepal can be obtained. The fracture surface morphology of all specimens were examined using the scanning electron microscope (SEM). Prior to SEM examination, all samples were coated by a vacuum-evaporated layer of gold for about 12 s at 10 mA.

RESULTS AND DISCUSSION

Molecular and Crystalline Microstructure

Microstructural characterizations of series 1 (samples A_1, B_1, and C_1) are summarized in Table II. Approximately the same percent crystallinity (W_c) and tie-molecule density were found for samples of series 1. The percent crystallinity associated with

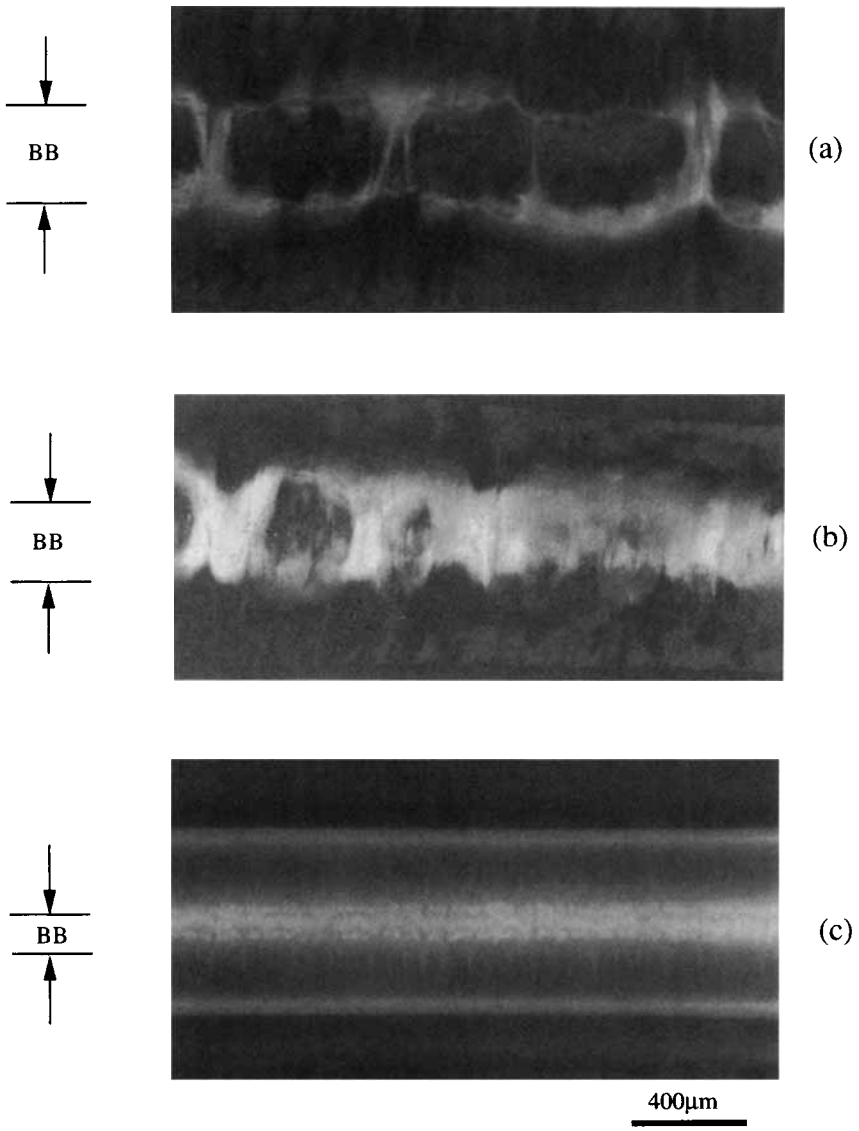

Figure 7 Optical views into root of notch of sample of series 1 in Igepal solution at 8.5 MPa after (a) 1040 min for sample A_1, (b) 960 min for sample B_1, and (c) 1100 min for sample C_1.

these samples was about 40%. As mentioned previously, tie-molecule densities were evaluated from their measured brittle fracture stress[26] and predicted from the chain dimensions[27] of the SBPE polymers. As shown in Table II, tie-molecule density (f_T) derived from measurement of brittle fracture stress was about 6% and the average number of tie molecules formed per chain [$T(M)$] for samples A_1, B_1, and C_1 was about 26. In addition to samples A_1, B_1, and C_1, samples A_2, A_3, B_2, B_3, C_2, and C_3 with different W_c were also prepared to study the possible effects of W_c on ITT and other environmental stress cracking properties of SBPE polymers in Igepal solution. Slightly higher W_c ($\sim$ 42 vs. $\sim$ 40%) was found for series 2 samples (i.e., A_2, B_2, and C_2) than that of samples of series 1 (i.e., A_1, B_1, and C_1). However, a significant decrease in W_c was found when samples of series 3 crystallized on quenching from the melt (i.e., samples A_3, B_3, and C_3). Percent crystallinities of samples A_3, B_3, and C_3 were around 27%. Approximately the same f_T and $T(M)$ were found for samples of series 1 and 2. However, a slightly increase in f_T and $T(M)$ were found when samples of series 3 were crystallized on quenching from the melt, which varied with the anticipated change in tie-molecule density, i.e., tie-molecule

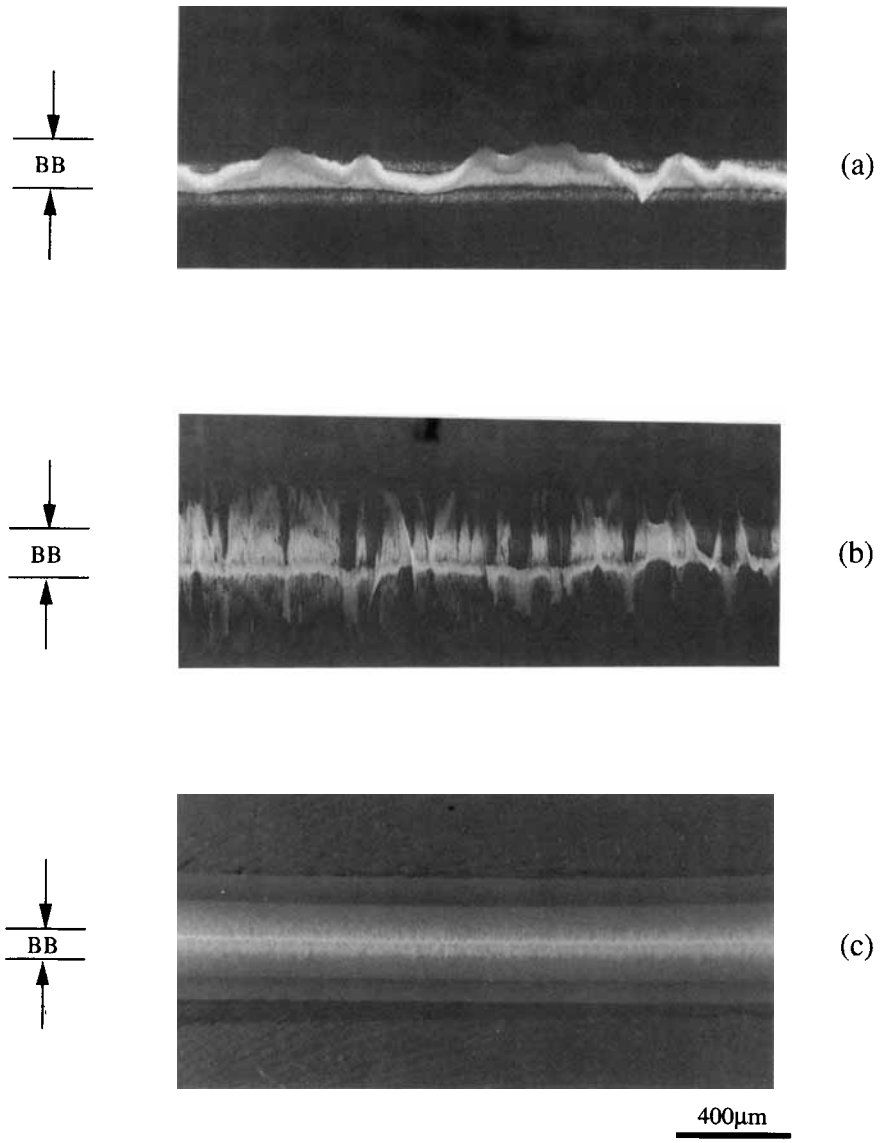

Figure 8 Optical views into root of notch of sample of series 1 in air at 8.5 MPa after (a) 980 min for sample A_1, (b) 870 min for sample B_1, and (c) 1080 min for sample C_1.

density increases on quenching and with increasing molecular weight. Similar to that of series 1 samples, approximately the same W_c and tie-molecule density was found with the two series of samples (i.e., series 2 and series 3 samples), respectively.

Environmental Stress Cracking Experiments

The curves of notch opening displacements (NOD) against time for sample A_1 fractured in air and in Igepal solution at 9 MPa are shown in Figure 3. The kinetics of damage of sample A_1 in air and Igepal solution were nearly the same. The NODs grew instantly upon loading the specimens in air and in Igepal solution, and then grew at a slow and nearly constant rate up to a critical value (δ_c), at which fibril fracture occurred. Beyond that point, the remaining ligament yielded prior to ultimate failure. Similar time dependence of the NODs of samples B_1 and C_1 loaded at 9 and 9.5 MPa in air and in Igepal solution was found, respectively. However, the kinetics of damage of samples of series 1 in Igepal solution was significantly different from those fractured in air as the load decreased. As shown in Figure 4, the kinetics of damage of samples of series 1 loaded at 8.5 MPa in Igepal solution was nearly the same

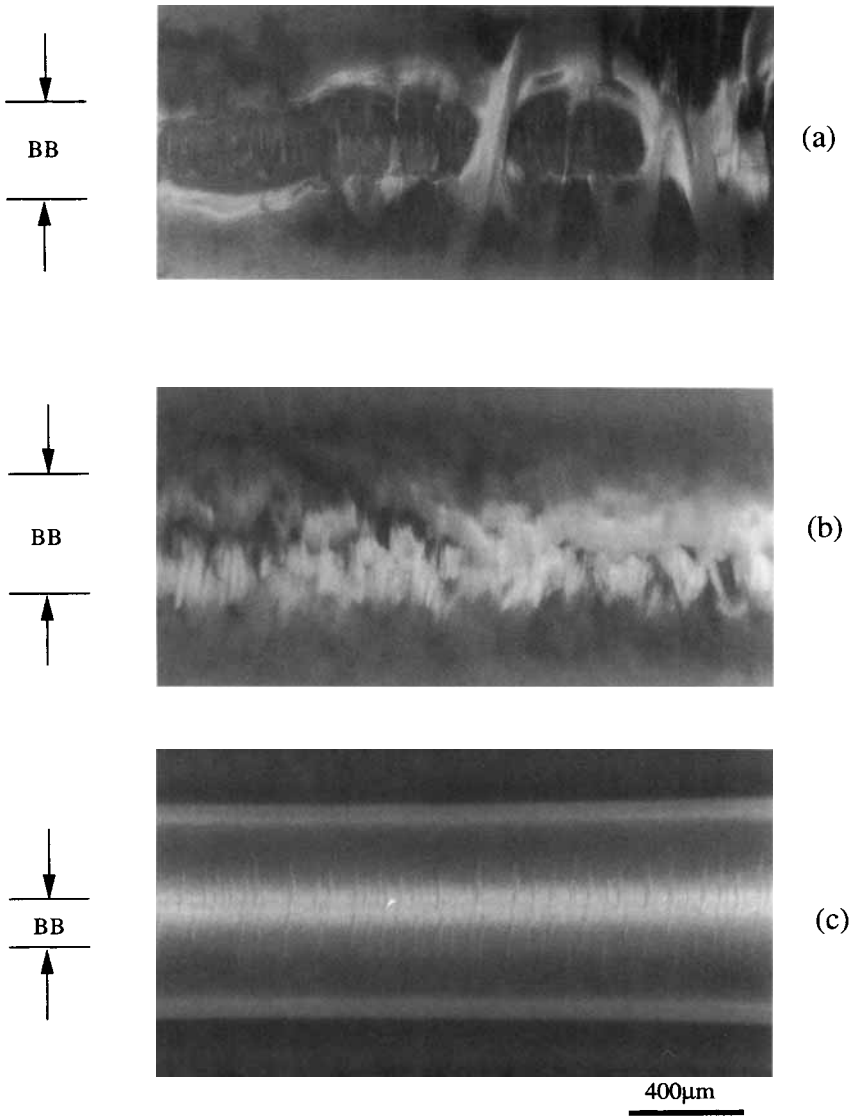

Figure 9 Optical views into root of notch of sample of series 2 in Igepal solution at 8.5 MPa after (a) 1080 min for sample A_2, (b) 1080 min for sample B_2, and (c) 1370 min for sample C_2.

as that in air at time before a critical time (about 1000 min). However, after the critical time, the growth rates of the notch openings in Igepal solution accelerated and resulted in a shorter failure time in Igepal solution (t_{fI}) than that in air. This critical time obtained in our study was first reported by Ward and co-authors[10] and was referred to as the Igepal transition time (ITT) in their study. As shown in Table III, it is interesting to note that ITTs of samples B_1 and C_1 were approximately the same as that of sample A_1 at the same loading condition. As described previously, samples of series 1 are associated with approximately the same molecular weight, molecule weight distribution, branch frequency, W_c, tie-molecule density, but different branch lengths. These results may imply that branch length has no effect on ITTs of SBPEs. In contrast, no ITT was found for samples A_1, B_1, and C_1 loaded at higher stresses (see Table III). This is probably due to the fact that Igepal required a certain amount of time to accelerate the fracture of SBPEs, and since t_{fI} associated with samples A_1, B_1, and C_1 at higher stresses is shorter than 1000 min and, hence, no acceleration of the growth rates of notch openings and no ITT can be observed.

On the other hand, it is interesting to note that t_{fI} and ESCR increased significantly as the short-chain branch length increased from 2 to 4 and 6

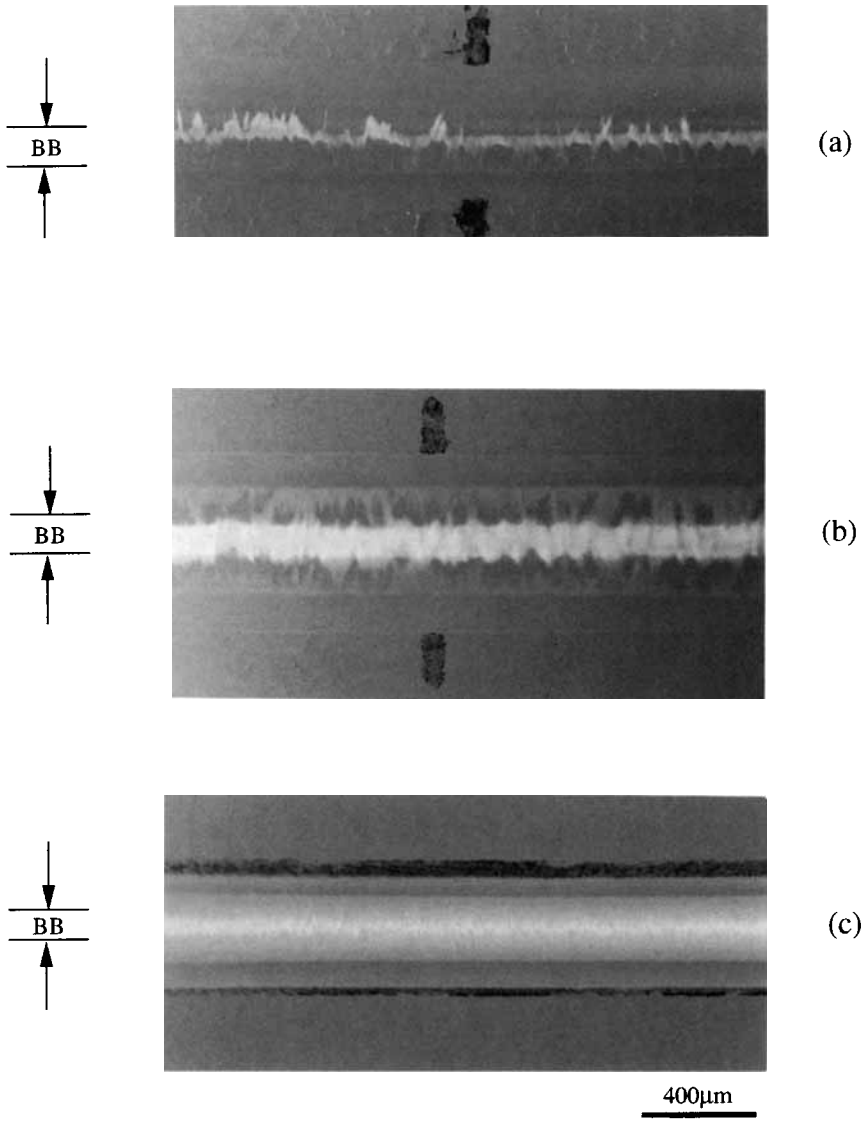

Figure 10 Optical views into root of notch of sample of series 2 in air at 8.5 MPa after (a) 980 min for sample A_2, (b) 880 min for sample B_2, and (c) 880 min for sample C_2.

carbon lengths. For example, t_{fl} of samples A_1, B_1, and C_1 at 8.5 MPa increased from 1300 to 2000 and 17000 min, respectively (see Fig. 5 and Table III). In fact, the improved t_{fl} and ESCR due to longer branch length continued at time after ITT. Similar branch length dependence of t_{fl} and ESCR was also found in samples of series 2 and 3. As mentioned previously, the weight-average molecular weight, molecular weight distribution, branch frequency, tie-molecule density, and W_c within each series (i.e., series 1, 2, and 3) remained approximately the same. Thus, the improved ESCR and t_{fl} is suggested to be due to the increasing branch length, which is believed to increase the sliding resistance of the polymer chains through the crystal and through the entanglement in amorphous region at time before and after ITT.

In samples A_2 and A_3 fractured in air and in Igepal solution at 8.5 and 8 MPa are interesting to note that the values of ITT and t_{fl} changed significantly when samples were associated with different W_c. As shown in Table III and Figure 6, the values of ITT and t_{fl} at 8.5 MPa increased from 510–640 to 1040–1280 and 1060–1530 min as W_c of sample A series increased from 26 to 40 and 42%, respectively (i.e., from A_3 to A_1 and A_2). Similar crystallinity depen-

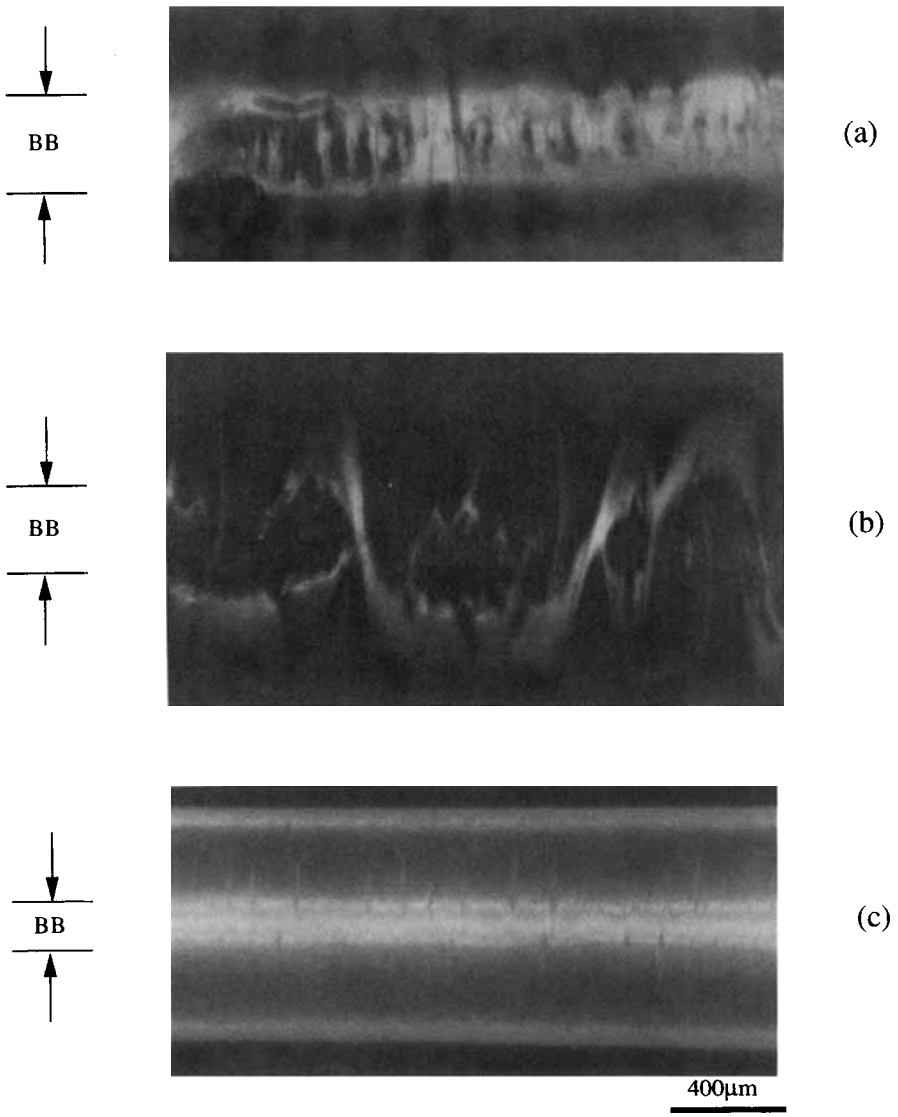

Figure 11 Optical views into root of notch of Sample of series 3 in Igepal solution at 8.5 MPa after (a) 580 min for sample A_3, (b) 440 min for sample B_3, and (c) 570 min for sample C_3.

dence of ITT and t_{fl} was found in sample B series (i.e., from B_3 to B_1 and B_2) and sample C series (i.e., from C_3 to C_1 and C_2) (see Fig. 6). Detailed mechanisms accounting for this significant increase in ITT and t_{fl} with W_c are not completely clear at this point. A possible role that W_c can play in improving the ESCR of SBPEs in Igepal solution is proposed as follows. It can be imagined that Igepal enhances crazing by plasticizing the amorphous regions first and required a certain amount of time to diffuse to the crystalline regions and then accelerate the fracture of SBPEs upon loading the specimens. Igepal may become more difficult to diffuse to the crystalline region and accelerate fracture of SBPEs as W_c increases since the crystalline and intercrystalline regions may become more perfect as polymers crystallized at higher temperatures rather than on quenching. Therefore, longer ITT and t_{fl} of SBPE polymers were observed for samples associated with higher W_c, and no significant difference in the values of ITTs was found when samples were with the same W_c even though they were associated with different short-chain branch lengths.

Morphology of the Notched Roots and Fracture Surface Analysis

The morphological changes at the root of all samples in Igepal solution and in air are shown in Figures

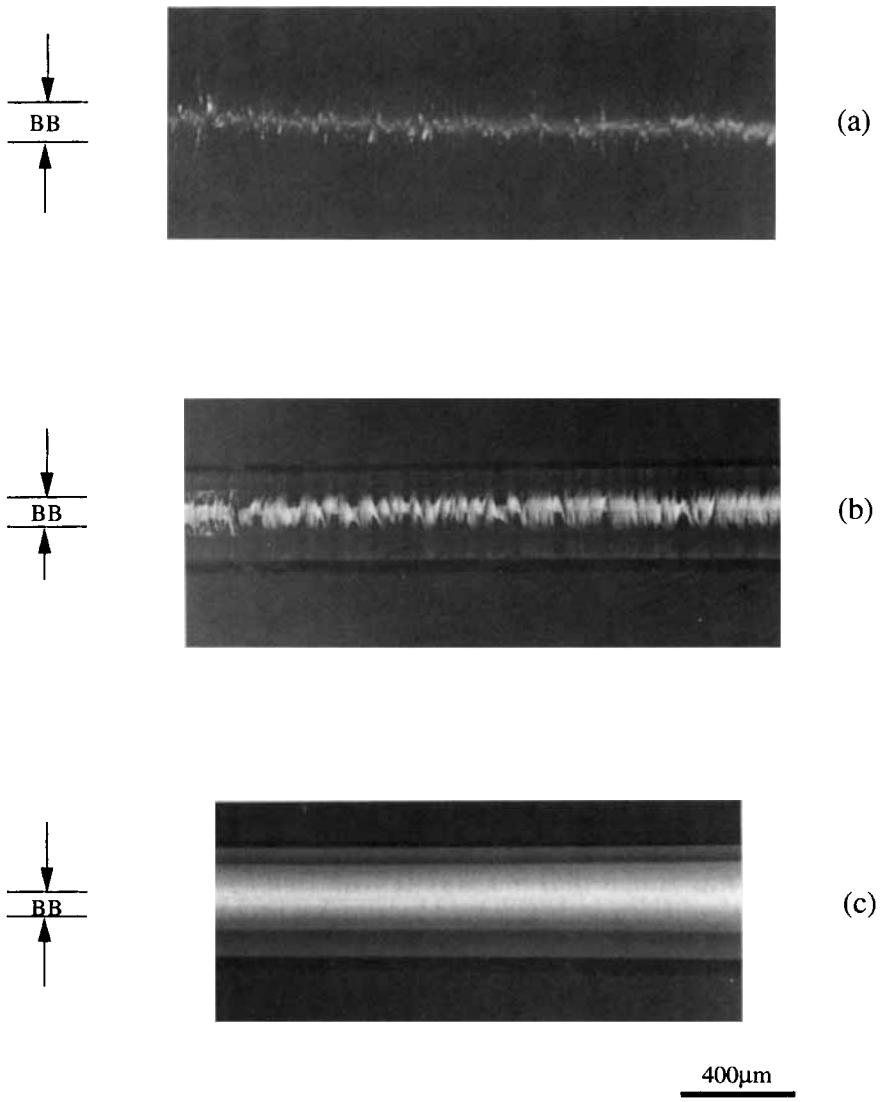

Figure 12 Optical views into root of notch of sample of series 3 in air at 8.5 MPa after (a) 510 min for sample A_3, (b) 430 min for sample B_3, and (c) 470 min for sample C_3.

7–12. Views of the NODs upon looking into the middle of the notch are observed on each figure where the base of the craze appears as a bright zone under the reflected light, which suggests that the crazing mechanism occurs in any of these materials regardless of testing conditions (i.e., air or Igepal solution). However, at time near ITT, "enlarged" voids appeared in the base of the craze in Igepal solution, the film was then shred and completely damaged before ultimate failure (see Figs. 7, 9, and 11). In contrast, similar enlarged voids were not found in those of samples fractured in air (see Figs. 8, 10, and 12). These results suggests that the Igepal solution at the lower stresses accelerates and possibly enhances this crazing and voiding process.

The fracture surfaces of sample A_1 fractured in air and in Igepal solution at 8.5 MPa are shown in Figures 13(a) and (b), respectively. In all of these micrographs, the direction of crack propagation is from left to right and is perpendicular to the front notch (as shown in Fig. 1). During the early stages of notch opening, no significant difference in the feature of the fracture surface was found for sample A_1 fractured in air and in Igepal solution. As the crack length increased, several crazelike structures containing clear voids were found on the fracture remnants of the sample, which cannot be found on that of sample A_1 fractured in air at 8.5 MPa. Similar crazelike structures were also observed on the fracture surfaces of samples B_1 and C_1 damaged at the same load in Igepal solution (see Figs. 14–15). In fact, the voids contained in the crazelike structure tended to enlarge for samples associated with longer t_{fl} (i.e., longer branch length). However, no enlarged voids contained in crazelike structures were found on the fracture remnants of samples A_1, B_1, and C_1 loaded at higher stresses in Igepal solution, which were associated with a t_{fl} shorter than their ITT ($\sim$ 1000 min). Similar to that of series 1 samples, some enlarged voids contained in crazelike struc-

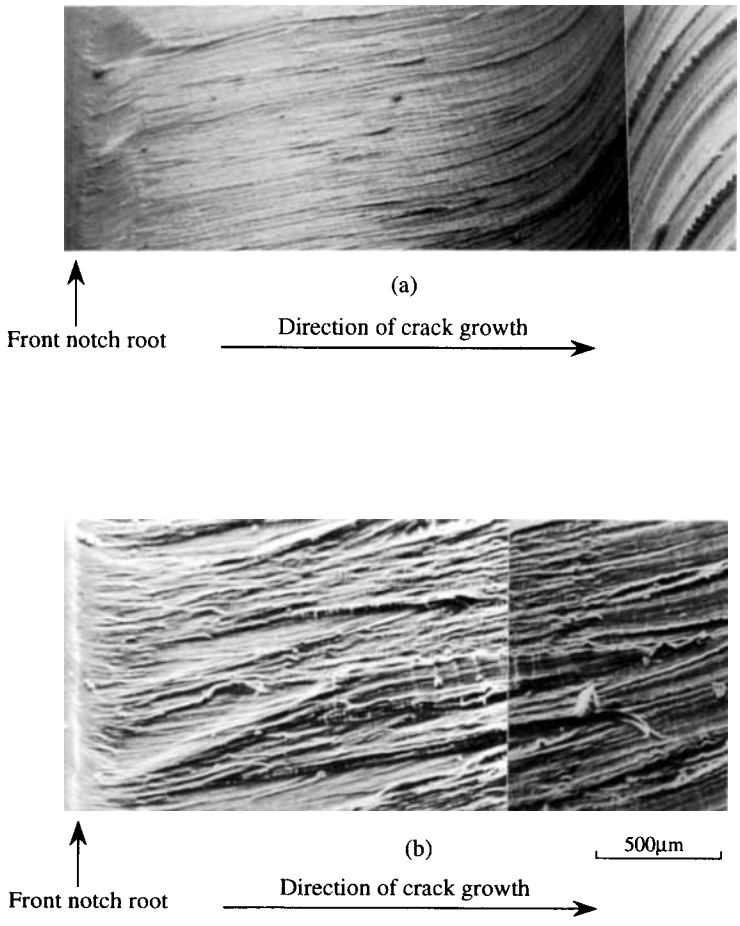

Figure 13 Fracture surfaces of sample A_1 fractured (a) in air and (b) in Igepal solution at 8.5 MPa.

tures were observed on the fracture surfaces of samples of series 2 and 3 as long as t_{fI} is long enough to make Igepal "effective" to accelerate fracture of SBPEs in Igepal solution. These enlarged voids observed in the base of craze and on the fracture surfaces can be due to the "effective diffusion" of Igepal solution in SBPE polymers, and, hence, accelerating the fracture of SBPEs.

CONCLUSION

The precise value of ITT and the difference between the failure process of SBPEs in air and in Igepal solution were determined by comparing their plots of NODs vs. time in air and in Igepal solution. ITT can only be found as t_{fI} is greater than the critical time Igepal required to "accelerate" the fracture of SBPEs. Prior to ITT, time dependence of NODs and fracture surfaces of samples in Igepal solution were similar to those in air. In contrast, obvious voids appeared in the base of craze and on the fracture remnants of samples with t_{fI} longer than their ITT. On the other hand, the values of ITT and t_{fI} were found to increase significantly for samples associated with higher W_c. It is believed that Igepal may become more difficult to diffuse to the crystalline region and accelerate the fracture of SBPEs in Igepal solution as W_c increases since the crystalline and intercrystalline regions may become more perfect as polymers crystallized at higher temperatures rather than on quenching. Finally, it is interesting to note that no significant difference in value of ITT was found for samples with the same W_c, tie-molecule density, molecular weight, branch frequency but different branch length (i.e., A_1, B_1, and C_1). However, ESCR and t_{fI} increased dramatically as the short-chain branch length increased from 2 to 4 and 6 carbon lengths (i.e., from A_1 to B_1 and C_1). This improvement in ESCR and t_{fI} is attributed to

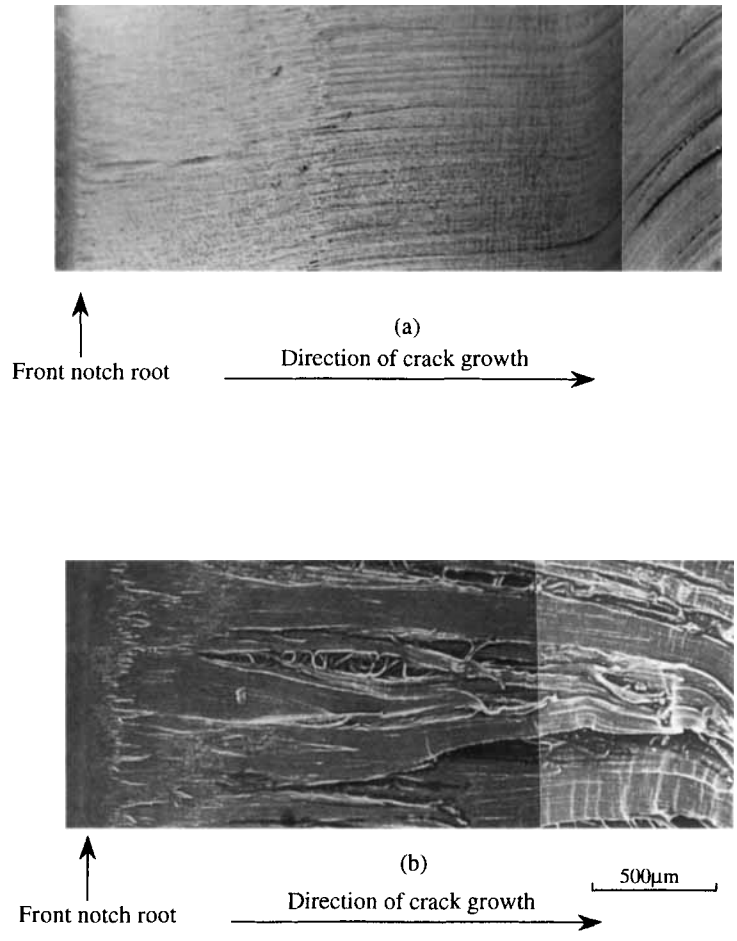

Figure 14 Fracture surfaces of sample B_1 fractured (a) in air and (b) in Igepal solution at 8.5 MPa.

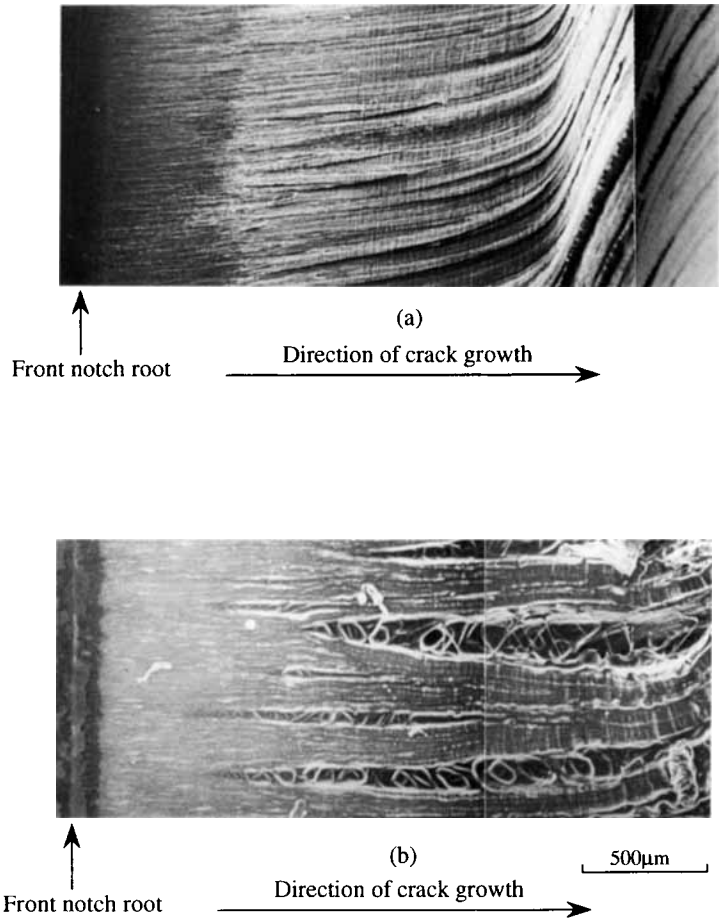

Figure 15 Fracture surfaces of sample C_1 fractured (a) in air and (b) in Igepal solution at 8.5 MPa.

the increasing sliding resistance of the polymer chains through the crystal and through the entanglement in amorphous region at time before and after ITT.

The authors express their appreciation to the National Science Council (Grant NSC 82-0405-E011-142) for support of this work. Thanks are also extended to Misses Hui-Mei Yang, Hsiu-Chuan Hsieh, and Mr. Yu-Lang Lin for their assistance in preparation of this manuscript.

REFERENCES

1. X. Lu, X. Q. Wang, and N. Brown, *J. Mater. Sci.*, **23,** 643 (1988).
2. X. Lu and N. Brown, *J. Mater. Sci.*, **21,** 2423 (1986).
3. Y. L. Huang and N. Brown, *J. Polym. Sci., Polym. Phys. Ed.*, **28,** 2007 (1990).
4. F. M. Mirabella, Jr., S. P. Westphal, P. L. Fernardo, E. A. Ford, and J. G. Williams, *J. Polym. Sci., Polym. Phys. Ed.*, **26,** 1995 (1988).
5. Y. L. Huang and N. Brown, *J. Polym. Sci., Polym. Phys. Ed.*, **29,** 129 (1991).
6. X. Lu and N. Brown, *J. Mater. Sci.*, **26,** 612 (1991).
7. J. T. Yeh, C. Y. Chen, and H. S. Hong, *J. Mater. Sci.*, to appear.
8. J. J. Strebel and A. Moet, *J. Mater. Sci.*, **26,** 5671 (1991).
9. A. L. Ward, X. Lu, and N. Brown, *Polym. Eng. Sci.*, **30,** 1175 (1990).
10. A. L. Ward, X. Lu, Y. Huang, and N. Brown, *Polymer*, **32,** 2172 (1991).
11. R. A. Bubeck and H. M. Baker, *Polymer*, **23,** 1690 (1982).
12. T. Hinton and A. Keller, *J. Appl. Polym. Sci.*, **13,** 745 (1969).
13. J. B. Howard, in *Crystalline Olefin Polymers, Part II*, R. A. V. Raff and K. W. Doak, Eds., Interscience, New York, p. 47, 1965.
14. M. De Pooter, P. B. Smith, K. K. Dohrer, K. F. Bennett, M. D. Meadows, C. G. Smith, H. P. Schouwen-

arrs, and R. A. Geerards, *J. Appl. Polym. Sci.*, **42,** 399 (1991).
15. B. Wunderlich, *Macromolecular Physics,* Vol. 1, Academic Press, New York, 1973, p. 388.
16. H. D. Keith, F. J. Padden, Jr., and R. G. Vadimsky, *J. Polym. Sci., Part A-2,* **4,** 267 (1966).
17. H. D. Keith, F. J. Padden, Jr., and R. G. Vadimsky, *J. Appl. Phys.*, **37,** 4027 (1966).
18. H. D. Keith, F. J. Padden, Jr., and R. G. Vadimsky, *J. Appl. Phys.*, **42,** 4585 (1971).
19. R. G. Vadimsky, H. D. Keith, and F. J. Padden, *J. Polym. Sci., Part A-2,* **7,** 1367 (1969).
20. H. A. Davis, *J. Polym. Sci., Part A-2,* **4,** 1009 (1966).
21. S. Hagou and K. Azuma, *J. Macromol. Sci., Phys. Ed.*, **16,** 435 (1979).
22. E. S. Clark, *S. P. E. J.*, **23,** 46 (1967).
23. H. D. Keith, F. J. Padden, Jr., and R. G. Vadimsky, *J. Polym. Sci., Polym. Phys. Ed.*, **18,** 2307 (1980).
24. E. W. Fischer, K. Hahn, J. Kugler, U. Struth, and R. Bom, *J. Polym. Sci., Polym. Phys. Ed.*, **22,** 1491 (1984).
25. V. V. Zhizhenkov and E. A. Egorov, *J. Polym. Sci., Polym. Phys. Ed.*, **22,** 117 (1984).
26. N. Brown and I. M. Ward, *J. Mater. Sci.*, **18,** 1405 (1983).
27. J. T. Yeh and J. Runt, *J. Polym. Sci., Polym. Phys. Ed.*, **29,** 371 (1991).

Received August 13, 1993
Accepted December 9, 1993